ANNALS of Clinical and Translational Neurology
Open Access
ANA American Neurological Association since 1875

RESEARCH ARTICLE

Central neuropathic pain in MS is due to distinct thoracic spinal cord lesions

Darin T. Okuda[1], Kara Melmed[2], Takashi Matsuwaki[3], Anders Blomqvist[3] & Arthur D. Bud Craig[4]

[1]UT Southwestern Medical Center, Department of Neurology & Neurotherapeutics, Clinical Center for Multiple Sclerosis, Dallas, Texas
[2]University of Arizona College of Medicine, Phoenix, 550 E. Van Buren, Phoenix, Arizona, 85004
[3]Division of Cell Biology, Department of Clinical and Experimental Medicine, Faculty of Health Sciences, Linköping University, Linköping, Sweden
[4]Atkinson Research Laboratory, Barrow Neurological Institute, 350 W. Thomas Road, Phoenix, Arizona, 85013

Correspondence
Darin T. Okuda, UT Southwestern Medical Center, Department of Neurology & Neurotherapeutics, Clinical Center for Multiple Sclerosis, 5323 Harry Hines Blvd., Dallas, TX 75390-8806. Tel: 214-645-0555; Fax: 214-645-0556;
E-mail: darin.okuda@UTsouthwestern.edu

Funding Information
The work in A. B.'s laboratory was supported by grants from the Swedish Research Council–Medicine (7879, 20535, 20725), the Swedish Brain Foundation, Konung Gustaf V: s 80-årsfond, and the County Council of Östergötland. The work in A. D. C.'s laboratory was supported by the James R. McDonnell Foundation and the Barrow Neurological Foundation.

Received: 22 April 2014; Revised: 3 June 2014; Accepted: 17 June 2014

Annals of Clinical and Translational Neurology **2014; 1(8): 554–561**

doi: 10.1002/acn3.85

Abstract

Objective: To determine a neuro-anatomic cause for central neuropathic pain (CNP) observed in multiple sclerosis (MS) patients. **Methods**: Parallel clinical and neuro-anatomical studies were performed. A clinical investigation of consecutively acquired MS patients with and without CNP (i.e. cold allodynia or deep hyperesthesia) within a single MS center was pursued. A multivariate logistic regression model was used to assess the relationship between an upper central thoracic spinal cord focus to central pain complaints. To identify the hypothesized autonomic interneurons with bilateral descending projections to lumbosacral sensory neurons, retrograde single- and double-labeling experiments with CTb and fluorescent tracers were performed in three animal species (i.e. rat, cat, and monkey). **Results**: Clinical data were available in MS patients with (n = 32; F:23; median age: 34.6 years (interquartile range [IQR]: 27.4–45.5)) and without (n = 30; F:22; median age: 36.6 years [IQR: 31.6–47.1]) CNP. The value of a central focus between T1–T6 in relation to CNP demonstrated a sensitivity of 96.9% (95% confidence interval [CI]: 83.8–99.9) and specificity of 83.3% (95% CI: 65.3–94.4). A significant relationship between CNP and a centrally located focus within the thoracic spine was also observed (odds ratio [OR]: 155.0 [95% CI lower limit: 16.0]; $P < 0.0001$, two-tailed Fisher exact test). In all animal models, neurons with bilateral descending projections to the lumbosacral superficial dorsal horn were concentrated in the autonomic intermediomedial nucleus surrounding the mid-thoracic central canal. **Interpretation**: Our observations provide the first evidence for the etiology of CNP. These data may assist with the development of refined symptomatic therapies and allow for insights into unique pain syndromes observed in other demyelinating subtypes.

Introduction

Central neuropathic pain (CNP) in multiple sclerosis (MS) is phenotypically heterogeneous.[1] Approximately 30–40% of patients with MS suffer from CNP; at times, focused symmetrically in both feet and legs, sometimes including the hands,[2] and initiated by cold stimuli or deep pressure. Such pain is debilitating, often unrecognized in clinical practice,[3] and refractory to conventional prescribed treatments. This condition resembles thalamic central pain, which also presents with dysfunctional pain and temperature sensations; however, thalamic pain is strictly contralateral.[4]

Unifying mechanisms for the etiology of CNP are unknown, although proposed causes include the disinhibition of pain signaling pathways within the dorsal column,[5] disruption of decussating fibers of spinothalamic tracts,[6] disinhibition of thermosensory integration,[4] and magnitude of gray matter involvement within the spinal cord.[7] Beyond structural causes, the immune system following neural injury with the complex interplay of immune and glial cells and inflammatory mediators may also be involved.[8]

A distinct explanation for bilateral MS central pain likely involves a spinal lesion in a discrete location that can produce bilateral effects, yet a correlation remains unidentified.[1] We hypothesized that the dense ascending projections from lumbosacral lamina I neurons to bilateral upper/mid-thoracic autonomic nuclei are mirrored by descending projections that modulate spinothalamic "pain and temperature" lamina I neurons,[9] comparable to the bidirectional connections between lamina I and autonomic pre-motor sites, such as A5, A6 and A7; thus, an upper/mid-thoracic lesion that damaged autonomic interneurons with bilateral descending projections to lumbosacral lamina I neurons might result in bilateral dysfunctional pain and temperature sensations, as observed in MS patients with central pain. Prior neuro-anatomical studies in cats revealed upper/mid-thoracic neurons in the autonomic cell columns that project to the lumbosacral spinal cord,[10,11] but did not identify the hypothesized interneurons with bilateral projections to the superficial dorsal horn. The overall goal of the investigation was to further explore this hypothesis through parallel clinical and neuro-anatomical studies in an effort to identify an anatomical association within the thoracic spinal cord parenchyma to CNP.

Methods

Clinical methods

Study participants

The cohort was ascertained through the systematic collection of MS cases from a single MS center. All cases of CNP were consecutively collected by a single MS specialist (D. T. O.), who was blinded, not only to the results from the neuroanatomical experiments but also to the findings on structural neuroimaging of the central nervous system prior to group assignment. Patients were included in the CNP group if the following criteria were met: (1) 18 years of age or older, (2) diagnosis of MS, (3) available imaging of the brain, cervical, and thoracic spinal cord, and (4) documentation of CNP as defined by the presence of bilateral lower extremity cold allodynia or deep hyperesthesia on neurological examination. Cold allodynia was assessed using a tuning fork at room temperature that was primed with alcohol prior to use. Deep hyperesthesia was assessed through manual pressure on the lower extremities. Patients were excluded if they possessed incomplete medical history or radiological data, or had a diagnosis other than MS (i.e. neuromyelitis optica, transverse myelitis, etc.).

Patients who possessed similar comprehensive imaging of the central nervous system CNS, who were evaluated during the same day of clinical service, and lacked specific CNP complaints of cold allodynia and deep hyperesthesia were also consecutively collected. Sensory complaints other than cold allodynia or deep hyperesthesia were allowed within the non-CNP group (i.e. paresthesias, burning, etc.). In all cases, data from a detailed clinical history, comprehensive neurological evaluation, para-clinical and imaging studies were available for review. An Institutional Review Board-approved research protocol was used for this study.

Structural neuro-imaging

All patients included had magnetic resonance imaging (MRI) studies of the brain, cervical, and thoracic spine performed within a 30-day period. The sequences were acquired through nonuniform protocols at magnetic field strengths of 1.5 Tesla (T) or 3.0 T performed at multiple academic and community institutions, yielding MRI studies containing images with varying signal-to-noise ratios, slice thicknesses, and gaps between acquired images. All examinations included T1 and T2-weighted spin-echo sequences in multiple planes of view (axial, coronal, and sagittal) with and without the administration of gadolinium. A short-time inversion recovery (STIR) sequence was available for all MRI studies of the cervical and thoracic spinal cord.

For all structural neuro-imaging studies reviewed, abnormalities within the brain or spinal cord were initially identified by a neuro-radiologist on the formal interpretation and subsequently verified by an MS specialist (D. T. O.). A qualitative (i.e. geographical positioning and morphology of lesions) and quantitative (i.e. number of T2-foci, presence or absence of gadolinium enhancement) analysis of the available brain spinal cord imaging studies was performed on all study participants.

Brain MRI studies were assessed for the presence of lesions in the supratentorial and infratentorial regions, with specific attention to brainstem structures and the presence of gadolinium enhancement. Lesions within the cervical and thoracic spinal cord were deemed significant if the following criteria were met: (1) focal or multi-focal involvement of the spinal cord parenchyma with ovoid, well-circumscribed lesions present, (2) noncontiguous lesions involving $\leq$2 spinal segments, (3) abnormalities present on more than 1 MRI sequence and/or plane of view, and (4) the high-signal abnormalities were not better accounted for by another process (i.e. protruding disc, vascular malformation, etc.).

Statistical analysis

All calculations and statistical analyses were performed using Stata/IC 12.0 (Stata Corporation, College Station, TX).

Chi-square tests were used to assess statistically significant differences between groups with and without CNP. Medians with interquartile ranges (IQR) (25th–75th percentiles) were acquired to summarize the demographic, clinical, and radiological data.

The significance of the presence of a thoracic demyelinating plaque located centrally within the thoracic spinal cord (T1–T6) in predicting CNP was determined by calculating the true positives (MS patients with a T1–T6 centrally positioned lesion with CNP), false positives (MS patients with a T1–T6 centrally positioned lesion with no complaints of CNP), true negatives (MS patients without a T1–T6 centrally positioned lesion and no central pain), and false negatives (MS patients without a T1–T6 centrally positioned lesion but developing CNP). The sensitivity (true positives/[true positives + false negatives]) and specificity (true negatives/[true negatives + false positives]) was also calculated with corresponding confidence 95% confidence intervals (CI). A two-tailed Fisher exact test was used for analysis of the contingency table with odds ratios (ORs), 95% CI, and *P* values calculated.

A demyelinating plaque located centrally within T1–T6 was used as the primary predictor in logistic regression models to assess the outcome of CNP. Covariates include the following: age at MS diagnosis, age at first clinical symptom, disease duration from the time of diagnosis and first symptom, race/ethnicity, sex, family history for MS, presence of contrast enhancement on MRI scans, presence of posterior fossa lesions, presence of brainstem lesions, presence of cervical spine disease, spinal cord lesion number, thoracic spine involvement (T7–T9; T10–T12), abnormal cerebrospinal fluid profiles (elevated IgG index [>0.70] or the presence of >2 unique oligoclonal bands within the central nervous system), and exposure to disease modifying therapy. Meaningful covariates were incorporated into the multivariate logistic regression model, generating ORs and 95% CI and *P* values. Continuous predictors of age and disease duration were assessed for normality via measures of skewness and kurtosis. Multicollinearity among predictors was also assessed by examination of standard errors of parameter estimates.

A P value ≤ 0.05 was considered significant.

Neuroanatomical methods

Animal experiments

The experiments were authorized by the appropriate local authorities (rats in Linköping, cats and monkey in Phoenix). All animals were deeply anesthetized for all procedures. Animals were mounted in a spinal frame, and the lumbosacral enlargement was exposed by dorsal laminectomy. In 2 rats, a micropipette was inserted just below the left L5 pia mater and 100 nL of the tracer cholera toxin subunit B (CTb; 1%, List Biological, Campbell, CA) was pressure injected, as before.[12] In cat-1, a 10 μL syringe was inserted into left S1 and L7 longitudinally at a steep angle and 1 μL CTb was slowly injected as it was withdrawn. In cat-2, a micropipette inserted 700 μm vertically into left L7 (at the medial edge of the dorsal root entry zone) was used to make three 100 nL pressure injections of CTb spaced at 0.5 mm rostro-caudal intervals. In cat-3, a 10 μL syringe inserted vertically was used to make three rostro-caudally spaced injections of 10K dextran conjugated to Alexa546 (10%, Invitrogen, Grand Island, NY) at depths of 500–1000 μm in left L7-S1, and on the right side three injections were made similarly of 10K dextran conjugated to Lucifer Yellow (10%, Invitrogen, Grand Island, NY). In cat-4, such double injections were made on the opposite sides. In monkey-1, five pressure injections of 200 nL Alexa546-dextran(10K) each were made with a micropipette at depths of 500–700 μm in the left superficial L7 dorsal horn at 0.5 mm rostro-caudal intervals.

All animals survived an appropriate time for axonal transport (rat, 3 days; cat, 8–28 days; monkey, 11 days) and then were deeply anesthetized and perfused transcardially with fixative, as before.[12,13] Frozen transverse or horizontal 50 μm-thick sections were processed for CTb immunohistochemistry as before; sections containing fluorescent tracer were mounted and examined with appropriate epi-microscopic filters. Plots were made manually using a camera lucida. Photomicrographs were made with a Nikon DS-Ri1 or DS-F1 digital camera (Tokyo, Japan); sharpness, brightness, and contrast were adjusted using Adobe Photoshop.

Results

Clinical data

The clinical arm of the investigation involved the consecutive acquisition of 32 patients (women: 23 (73%); median age at MS diagnosis: 34.6 years [IQR: 27.4–45.5]) with a significant history for bilateral lower extremity cold allodynia or deep hyperesthesia and confirmed CNP findings (i.e. bilateral cold allodynia or deep hyperesthesia) on neurological examination. All subjects with CNP screened were included within the study and none were excluded. Age and sex matched MS patients ($N = 30$; women: 22 [73%]; median age at MS diagnosis: 36.6 years [IQR: 31.6–47.1]) lacking bilateral CNP complaints served as the control group. Table 1 summarizes the demographic data of the study cohort.

Table 2 summarizes both the clinical and radiological characteristics of patients. A higher number of cases with

Table 1. Demographic data of multiple sclerosis patients with and without central neuropathic pain.

	(+) Central neuropathic pain	(−) Central neuropathic pain
Cohort	*N* = 32	*N* = 30
Median age, years (interquartile range)		
MS diagnosis	34.6 (27.4–45.5)	36.6 (31.6–47.1)
First clinical symptom	33.2 (23.1–44.3)	35.9 (27.81–44.05)
Sex, female (%)	22 (69)	22 (73)
Race/Ethnicity, No. (%)	White, 26 (81.3)	White, 22 (73.3)
	African American, 2 (6.3)	African American, 1 (3.3)
	Hispanic, 4 (12.5)	Hispanic, 5 (16.7)
		Native American, 1 (3.3)
		Middle Eastern, 1 (3.3)

thoracic spinal cord involvement were observed in the group with CNP (97% vs. 50%; $P < 0.001$). Significant differences with respect to the presence of a centrally positioned demyelinating focus (Fig. 1A) versus a non-centralized lesion (Fig. 1B) within the thoracic spine (97% vs. 20%; $P < 0.001$) along with a higher likelihood of involvement within the upper/mid-thoracic spine (97% vs. 20%; $P < 0.001$) were also observed (Fig. 1A and C).

The value of a centrally located focus within the thoracic spinal cord between T1–T6 in relation to CNP complaints was determined with an observed sensitivity of 96.9% (95% CI 83.8–99.9) and specificity of 83.3 (95% CI 65.3–94.4). A statistically significant relationship between CNP and the presence of a centrally located demyelinating focus within the thoracic spine (OR = 155.0 [95% CI lower limit 16.0]; $P < 0.0001$, two-tailed Fisher exact test) was also identified.

The multivariate logistic regression model incorporating meaningful covariates supported this observation with a substantial increase in the odds of developing CNP observed when a central demyelinating focus within the upper/mid-thoracic spinal cord (T1–T6) was present (OR 155.0, 95% CI 17.0–1414.0, $P < 0.001$). A sensitivity analysis was performed to assess the impact of other covariates with no significant changes in statistical outcomes demonstrated.

Neuroanatomical data

Our neuroanatomical studies used standard retrograde labeling techniques to identify neurons in the thoracic spinal segments with descending projections to the superficial dorsal horn of the lumbosacral enlargement in two rats, one monkey, and four cats. In all cases, labeled thoracic neurons were observed on both sides mainly in lamina I, lamina V, the intermediate zone and the ventral horn, consistent with prior reports in cats[10,11] with pronounced labeling in the thoracic autonomic nuclei, that is, the intermediolateral (IML) and intermediomedial (IMM) cell columns. In all cases, the thoracic labeling in lamina I and the IML was predominantly ipsilateral, whereas labeling in the IMM was bilateral with a contralateral emphasis.

In both rats, the small injection in left L5 was limited to lamina I, and it produced clusters of labeled thoracic IMM cells dorsal to the central canal (Fig. 2A).

Table 2. Clinical and radiological characteristics of MS patients with and without central neuropathic pain.

	(+) Central neuropathic pain	(−) Central neuropathic pain
Multiple sclerosis subtype:		
Relapsing-remitting, No. (%)	22 (68.8)	26 (86.7)
Secondary-progressive, No. (%)	8 (25)	2 (6.7)
Primary progressive, No. (%)	2 (6.3)	2 (6.7)
Disease duration, median age, years (interquartile range)	4.7 (2.6–12.7)	2.0 (0.8–6.7)
Clinical follow-up time, median age, years (interquartile range)	2.2 (0.55–4.7)	2.0 (0.55–5.1)
Brain MRI		
Presence of posterior fossa lesions, No. (%)	13 (41)	12 (40)
Presence of a demyelinating lesion within the medulla, No. (%)	0 (0)	0 (0)
MRI cervical spinal cord		
Presence of a cervical spinal cord lesion, No. (%)	25 (78)	22 (73)
Central cervical spinal cord focus, No. (%)	2 (6.3)	2 (6.7)
Number of cervical spinal cord lesions, median number (interquartile range)	3 (2–5)	2 (1–3)
MRI thoracic spinal cord		
Presence of a thoracic spinal cord lesion, No. (%)*	31 (97)	15 (50)
Central thoracic spinal cord focus, No. (%)*	31 (97)	6 (20)
MRI thoracic lesion (T1–T6), No. (%)*	31 (97)	5 (17)
Number of thoracic spinal cord lesions, median number (interquartile range)	2 (2–4)	1 (1–2)
Contrast enhancement present on MRI:		
Brain, No. (%)	4 (13)	3 (10)
Cervical spine, No. (%)	1 (3)	2 (7)
Thoracic spine, No. (%)	2 (6)	0 (0)
Abnormal cerebrospinal fluid profile, No. (%)	18 (56)	14 (47)
Exposure to DMT, No. (%)	29 (91)	23 (77)

MS, multiple sclerosis; MRI, magnetic resonance imaging; DMT, disease modifying therapy.
*$P < 0.001$.

Figure 1. Clinical Evidence. (A). Sagittal short time inversion recovery (STIR) MRI sequence of the thoracic spinal cord demonstrating a focus of hyperintensity at T1 in a 38-year-old man diagnosed with MS (1999) and central neuropathic pain, and axial T2-weighted gradient-echo (GRE) MRI of the T1 lesion demonstrating a central hyperintense focus within the upper thoracic spinal cord. (B). Sagittal STIR MRI of the thoracic spine demonstrating a focus of hyperintensity at T1 in a 40-year-old woman with demyelinating disease without central neuropathic pain, and axial T2-weighted turbo spin-echo MRI of the T1 lesion demonstrating a small hyperintense focus positioned at the right lateral aspect of the spinal cord. (C). Sagittal STIR MRI of the thoracic spinal cord demonstrating a central T2-hyperintense focus at T5–6. MRI, magnetic resonance imaging; MS, multiple sclerosis.

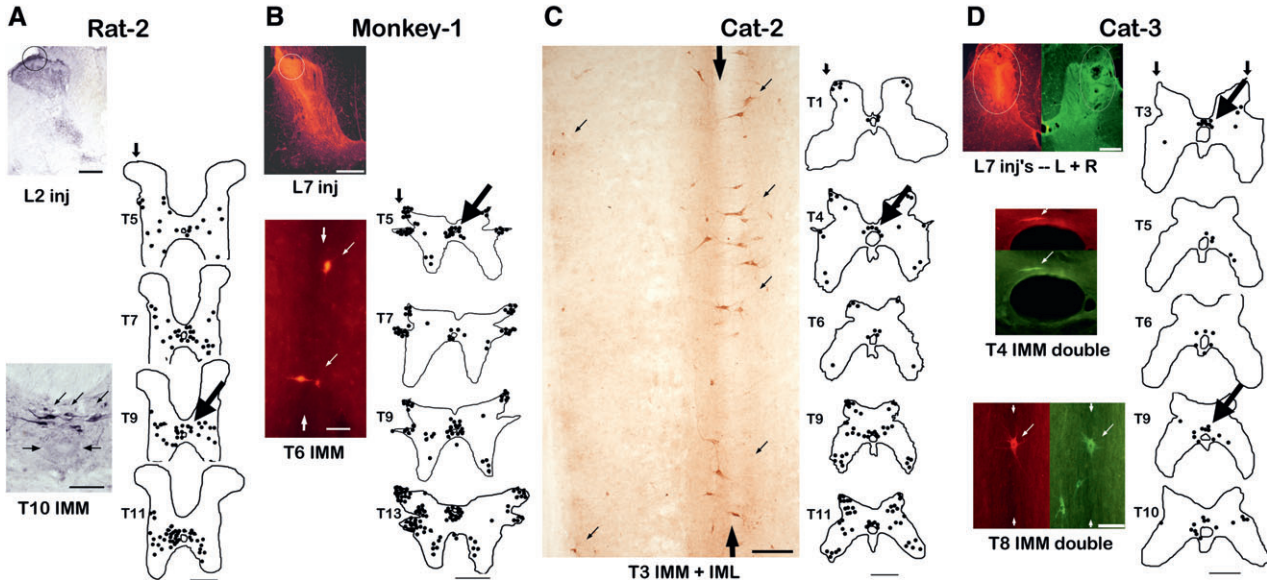

Figure 2. Neuroanatomical evidence. (A) An iontophoretic injection of CTb in lamina I of the left L5 segment in rat-2 produced retrogradely labeled neurons bilaterally in the intermediate zone and ventral horn of thoracic segments. The lower photomicrograph shows labeled IMM cells at T10 in a transverse section (lower arrows indicate the central canal). (B) Five pressure injections of 200 nL Alexa546-dextran(10K) each in the left superficial L7 dorsal horn of monkey-1 produced retrogradely labeled neurons concentrated in lamina I and the autonomic nuclei (IMM, intermediomedial; IML, intermediolateral) of thoracic segments. The lower photomicrograph shows labeled cells in the T6 IMM in a horizontal section (vertical arrows indicate the central canal). (C) Three pressure injections of 100 nL CTb each in the left superficial L7 dorsal horn produced retrogradely labeled neurons in lamina I, the IMM and the IML of thoracic segments in cat-2. The photomicrograph shows labeled cells in the ipsilateral T3 IML and IMM in a horizontal section (vertical arrows indicate the central canal). (D) Three pressure injections of 500 nL Alexa546-dextran(10K) each in the left L7 dorsal horn and of 500 nL LuciferYellow-dextran(10K) in the right L7 dorsal horn produced retrogradely double-labeled neurons concentrated in the IMM of thoracic segments. The lower photomicrographs show double-labeled cells in the T3 IMM (transverse) and the T8 IMM (horizontal; vertical arrows indicate the central canal).

In the monkey, small injections in the left L7 superficial dorsal horn produced retrograde labeling at thoracic levels that was strongly focused in lamina I, the IML and the IMM (Fig. 2B). In cat-1, a massive injection throughout left L7-S1 labeled thousands of thoracic neurons, whereas in cat-2 small injections in the superficial L7 dorsal horn labeled dozens, yet in both cases, concentrations of labeled neurons were observed in lamina I and the IML and IMM of thoracic segments (Fig. 2C).

In all cases, labeling gradually decreased from caudal to rostral thoracic levels, as expected,[10,11] yet there was

increased labeling in particular segments (see Table S1). The overall longitudinal distribution of labeling from the massive injection in cat-1 revealed strong concentrations of labeled neurons in the bilateral IMM of T1 and T5, the ipsilateral IML of T5, and ipsilateral lamina I of T1–2. The labeling patterns in the cases with small injections also indicate that the upper- and mid-thoracic segments are significant sources of descending input to the lumbosacral superficial dorsal horn, which mirrors the concentration of ascending lumbosacral lamina I projections to the autonomic nuclei in the same upper- and mid-thoracic segments.[14]

Finally, in two cats a red fluorescent tracer was injected in the L7 dorsal horn on the left side and a green fluorescent tracer was injected on the right side (or vice versa). Double-labeled neurons in both cases were located mainly in the thoracic IMM, dorsal to the central canal. A complete count obtained from segments T3 through T10 in cat-3 revealed that 61 of 83 double-labeled neurons (74%) were in the IMM, as shown in Figure 2D, with increased numbers in upper-thoracic segments T3–4.

Discussion

In this combined clinical and basic science research study, we identified a striking correspondence previously not described; MS patients with CNP are distinguished by the presence of a lesion focused in the center of the upper/mid-thoracic spinal cord, and neurons with bilateral descending projections to the lumbosacral superficial dorsal horn are concentrated in the autonomic IMM nucleus surrounding the central canal of the upper/mid-thoracic spinal cord.

The bilateral symptoms of cold allodynia and deep hyperesthesia in MS CNP patients are difficult to rationalize on the basis of a single lesion. A supratentorial lesion involving sensory pathways would primarily affect the contralateral side, as in the observed clinical phenotype in those with thalamic pain syndrome. A pathological focus within the brainstem affecting both sides symmetrically is plausible, but would likely be accompanied by concomitant clinical symptoms (i.e. motor involvement, cranial nerve abnormalities), given its dense structural organization. In addition, such an eloquently positioned lesion would be highly atypical. A spinal lesion affecting ascending lamina I spinothalamic fibers equally on both sides of the spinal cord could explain these symptoms, as previously noted,[2] but that also seems rather unlikely; ascending lamina I fibers course in the middle of the lateral funiculus,[9] and a lesion that affected these fibers on both sides symmetrically would encompass nearly the entire cross-section of the spinal cord, in effect producing a spinal transection and resulting in symptomatology extending beyond sensory pathways. Given these data, it seems more plausible that a lesion localized to the spinal cord has a greater propensity towards affecting ascending lamina I activity symmetrically on both sides if it disrupted descending modulation of ascending spinothalamic lamina I neurons bilaterally, resulting in dysfunctional "pain and temperature" sensibilities on both sides.

This hypothesis posits that interneurons exist which have bilateral descending projections to the lumbosacral superficial dorsal horn. Such interneurons have not been observed in prior studies. We considered the unique role that lamina I serves as the source of ascending homeostatic afferent activity in the hierarchically organized sensori-motor network that drives efferent autonomic activity.[14,15] Thus, lamina I projects to brainstem homeostatic integration sites (e.g., parabrachial nucleus, A1–2 and A5–7 groups, periaqueductal gray), and it receives complementary descending modulation from brainstem autonomic pre-motor sites (A5–7, raphe, ventromedial medulla) and from the paraventricular hypothalamus, which projects in the spinal cord only to the autonomic nuclei and lamina I.[16] At the bottom level of this hierarchy, lumbosacral lamina I neurons have dense, bilateral terminations in the upper/mid-thoracic autonomic cell columns[14]; we realized that, if these ascending sensory projections are also mirrored by descending bilateral projections to lumbosacral lamina I neurons, then a single MS lesion affecting autonomic interneurons with bilateral descending projections could produce dysfunctional modulation of ascending lamina I spinothalamic activity and, potentially, bilaterally symmetric pain and temperature symptoms.

In support of this hypothesis, we successfully identified and localized autonomic interneurons with bilateral descending projections to the lumbosacral superficial dorsal horn. Concurrently, and in a blinded fashion, we examined the geographical placement of lesions within the cervical and thoracic spine in MS patients with and without bilateral cold allodynia or deep hyperesthesia in the lower extremities. We identified a significant association between the presence of a central focus within the upper/mid-thoracic spinal cord and CNP. Some of the patients lacking CNP complaints possessed a history of neuropathic pain, however on neurological examination their sensory abnormalities (i.e. hyperesthesia, reduction in vibratory sensation, etc.) were found to be asymmetric and lacked exacerbating features with cold stimuli or deep pressure. In addition, these individuals lacked a centrally positioned focus involving the gray matter surrounding the central canal. The number of lesions within the spinal cord, presence of contrast enhancement within the brain or spinal cord, and involvement of the brainstem or cere-

bellar structures did not constitute significant predictors of risk for CNP.

Gray matter involvement within the central nervous system is commonly seen in MS patients.[17] The exact etiology of a central focus within the spinal cord, affecting myelinated gray matter axons, is unclear but likely results from the extravasation of inflammatory immune cells from central vein anastomoses that encircle the central canal. The extent of microarchitectural tissue involvement within lesions in MS is heterogeneous. However, despite the known heterogeneity with respect to the extent of axonal injury between foci identified in differing patients, and presumed varying degrees of insults to the descending autonomic projections, we observed well-defined structural involvement within the thoracic spinal cord on MRI only after obtaining a confirmed history of cold allodynia or deep hyperesthesia involving both lower extremities with verification of the symptomatic complaints on formal neurological examination. At present, the temporal profile for the development of CNP is unclear following the development of a centrally positioned focus within the thoracic spinal cord. Intuitively, a given threshold must exist for the development of CNP, whereby a given number of axons need to be compromised initially or following secondary degeneration. Despite the modest number of CNP MS patients, we were able to elicit bilateral lower extremity cold allodynia or deep hyperesthesia on neurological examination.

Future prospective, longitudinal, scientific efforts, involving a larger sample of CNP MS patients with comprehensive sensory mapping are needed to verify these data. In general, neuropathic pain complaints are common in those with MS, however CNP as specifically defined by the presence of bilateral cold allodynia and/or deep hyperesthesia is more rare. The use of high magnetic field strength and novel structural neuroimaging techniques, including diffusion tensor imaging and magnetization transfer imaging, may assist in our understanding of the heterogeneity of injury within lesions. In addition, the existence of similar connections within more rostral aspects of the spinal cord should be pursued.

The unanticipated and noteworthy observation of the association of centrally positioned upper/mid-thoracic spinal cord lesions to central pain, coupled with the neuroanatomical data provide strong evidence for the etiology of CNP, for which no explanation was previously available. Further anatomic insights into the cause of central pain in MS would generate both a greater understanding of nociception as well as encourage the development of therapeutic options. Our observations may lead to further advances in our understanding of the pathogenesis of central pain in MS but may also allow for insights into other unique pain syndromes observed in other demyelinating subtypes.

Acknowledgments

The work in A. B.'s laboratory was supported by grants from the Swedish Research Council–Medicine (7879, 20535, 20725), the Swedish Brain Foundation, Konung Gustaf V:s 80-årsfond, and the County Council of Östergötland. The work in A. D. C.'s laboratory was supported by the James R. McDonnell Foundation and the Barrow Neurological Foundation. Melmed and Matsuwaki, Blomqvist, and Craig have no conflicts of interest. Okuda received personal compensation for consulting, advisory board, and speaking activities from Acorda Therapeutics, Biogen IDEC, Genzyme, Novartis, and Teva.

Contributions

A. B., A. D. C., & T. M. performed the neuro-anatomical tracing experiments. A. D. C. & D. T. O. conceived and planned the experiments and wrote the paper. D. T. O. performed the statistical analysis of the clinical data.

Conflict of Interest

None declared.

References

1. Svendsen KB, Sorensen L, Jensen TS, et al. MRI of the central nervous system in MS patients with and without pain. Eur J Pain 2011;15:395–401.
2. Osterberg A, Boivie J, Thuomas KA. Central pain in multiple sclerosis–prevalence and clinical characteristics. Eur J Pain 2005;9:531–542.
3. Solaro C, Uccelli MM. Management of pain in multiple sclerosis: a pharmacological approach. Nat Rev Neurol 2011;7:519–527.
4. Craig AD. Mechanisms of thalamic pain. In: Henry JL, Panju A, Yashpal K, eds. Central Neuropathic Pain: Focus on Poststroke Pain. IASP Press, Seattle, WA: IASP Press, 2007. p. 81–100.
5. Foerster O. Die leitungsbahnen des schmerzgefühls und die chirurgische behandlung der schmerzzustände. Berlin: Urban and Schwartzenberg, 1927.
6. Osterberg A, Boivie J. Central pain in multiple sclerosis – sensory abnormalities. Eur J Pain 2010;14:104–110.
7. Finnerup NB, Gyldensted C, Nielsen E, et al. MRI in chronic spinal cord injury patients with and without central pain. Neurology 2003;61:1569–1575.

8. Calvo M, Dawes JM, Bennett DL. The role of the immune system in the generation of neuropathic pain. Lancet Neurol 2012;11:629–642.
9. Craig AD. How do you feel? Interoception: the sense of the physiological condition of the body. Nat Rev Neurosci 2002;3:655–666.
10. Yezierski RP, Culberson JL, Brown PB. Cells of origin of propriospinal connections to cat lumbosacral gray as determined with horseradish peroxidase. Exp Neurol 1980;69:493–512.
11. Matsushita M, Ikeda M, Hosoya Y. The location of spinal neurons with long descending axons (long descending propriospinal tract neurons) in the cat: a study with the horseradish peroxidase technique. J Comp Neurol 1979;184:63–80.
12. Ericson H, Blomqvist A. Tracing of neuronal connections with cholera toxin subunit B: light and electron microscopic immunohistochemistry using monoclonal antibodies. J Neurosci Methods 1988;24:225–235.
13. Craig AD. Retrograde analyses of spinothalamic projections in the macaque monkey: input to the ventral lateral nucleus. J Comp Neurol 2008;508:315–328.
14. Craig AD. Propriospinal input to thoracolumbar sympathetic nuclei from cervical and lumbar lamina I neurons in the cat and the monkey. J Comp Neurol 1993;331:517–530.
15. Craig AD, Zhang ET, Blomqvist A. Association of spinothalamic lamina I neurons and their ascending axons with calbindin-immunoreactivity in monkey and human. Pain 2002;97:105–115.
16. Holstege G. Direct and indirect pathways to lamina I in the medulla oblongata and spinal cord of the cat. Prog Brain Res 1988;77:47–94.
17. Kutzelnigg A, Lucchinetti CF, Stadelmann C, et al. Cortical demyelination and diffuse white matter injury in multiple sclerosis. Brain 2005;128(Pt 11):2705–2712.

Supporting Information

Additional Supporting Information may be found in the online version of this article:

Table S1. These tables show the numbers of labeled cells counted in serial horizontal or transverse sections of various spinal segments. In each set, all blocks were of similar longitudinal extent, unless noted otherwise. Labeled cells were counted in either lamina I (I), lamina V (V), the intermediate zone (VII), the ventral horn (VH), the intermediolateral (IML), or the intermediomedial (IMM) cell columns on both right and left. The two rats received an iontophoretic injection of CTb in lamina I of the left L5; cells were counted in 10 alternate sections from each segment. Monkey-1 received pressure injections of Alexa546-dextran(10K) in the left superficial L7 dorsal horn; the alternate transverse and horizontal blocks were each ~10 mm long. Cat-1 and cat-2 received large or small pressure injections of CTb in the left superficial L7 dorsal horn, respectively; all segments of cat-1 were sectioned horizontally (each ~18 mm long, except T1–2 and T3–4 were each ~12 mm), and the thoracic segments of cat-2 were alternately sectioned transverse (each ~ 10 mm long, except T6 was 5 mm) and horizontal (each ~20 mm long, except T2–3 was 13 mm). Cat-3 received pressure injections of Alexa546-dextran(10K) in the left L7 dorsal horn and LuciferYellow-dextran(10K) in the right L7 dorsal horn, and all double-labeled cells were counted; all segments were sectioned horizontally except T4, which was half as long and was cut transverse. Note that CTb is the most efficient retrograde tracer available for spinal labeling.[15]

